Star formation histories of Brightest Group Galaxies in CLoGS

O C Havenga[1], S I Loubser[1], E O'Sullivan[2], A Babul[3] and A Ratsimbazafy[1]

[1] Centre for Space Research, North-West University, Potchefstroom, 2520, South Africa
[2] Harvard-Smithsonian Centre for Astrophysics, 60 Garden Street, Cambridge, MA 02138
[3] Department of Physics and Astronomy, University of Victoria, Victoria, BC V8P 1A1, Canada

E-mail: `24909629@nwu.ac.za`

Abstract. An important component of galaxy formation and evolution studies, is to accurately constrain the star formation histories (SFHs) of galaxies. While the SFHs of most massive early-type galaxies can be described using a single passively-evolving stellar component (Single Stellar Population [SSP]), there is a fraction of massive early-type galaxies in the centres of galaxy groups and galaxy clusters where recent star formation is observed and are better described by two or more stellar components (Composite Stellar Population [CSP]). In this project we identify and constrain possible recent star formation episodes in a sample of 23 BGGs (Brightest Group Galaxies), which is a sub-sample of the Complete Local-Volume Groups Sample (CLoGS). Most of these BGGs are in the centres of X-ray rich groups and all are closer than 80Mpc. We use archival spatially-resolved long-slit spectroscopy from the Hobby-Eberly Telescope (HET) at the McDonald Observatory, and determine whether the BGGs are better described by an SSP or a CSP using ULySS. For this, stellar population models were fit to each of the 23 galaxies. The results showed that 11 of the BGGs were better described by a CSP while 12 of the BGGs were better described by an SSP. These results must be compared to the existing X-ray and radio observations of the groups.

1. Introduction

Galaxy groups are some of the best environments for studying the impact of galaxies on the surrounding Intergalactic Medium, as is done in [1].

The CLoGS sample is an optically selected sample of 53 galaxy groups within 80 Mpc. The sample selection is described in detail in [2]. X-ray, radio and sub-mm data have been collected for the entire sample [2]. In addition, [3] have analysed spatially-resolved long-slit spectroscopy from the 10m Hobby-Eberly Telescope (HET at the McDonald Observatory observed in September 2010 [4]) for a sub-sample of 23 BGGs. This project is a continuation, and uses the same sub-sample and data to derive star formation histories for the 23 BGGs. The aim is to study various properties of BGGs that serve as signatures of their evolutionary paths and also interpret the influence of the environment. The central galaxies (or BGGs) are in the centres of the groups' massive dark matter haloes and are thus ideal probes of galaxy evolution.

Table 1 gives information about the galaxies in this sub-sample. The sample was divided into two categories: a high-richness category and a low-richness category. [2] defined a richness parameter (R) as the number of galaxies within that group (within 1 Mpc from the centre and 3σ

in velocity of the BGG) with the luminosity constraint: $\log L_B \geq 10.2$. Groups with $4 \leq R \leq 8$ were classified as High-richness groups and groups with $R =$ 2-3 were classified as Low-richness groups.

Table 1. The basic information of the BGGs that are studied in this project.

Galaxy information				
High-richness				
Galaxy	**Redshift**	**RA**	**DEC**	**Velocity (km/s)**
NGC0410	0.0177	01h10m58.9s	+33d09m07s	5294
NGC0584	0.0060	01h31m20.7s	–06d52m05s	1802
NGC0777	0.0167	02h00m14.9s	+31d25m46s	5015
NGC0924	0.0149	02h26m46.8s	+20d29m51s	4461
NGC1060	0.0173	02h43m15.0s	+32d25m30s	5190
NGC1453	0.0130	03h46m27.2s	–03d58m08s	3886
NGC1587	0.0123	04h30m39.9s	+00d39m42s	3694
NGC2563	0.0149	08h20m35.7s	+21d04m04s	4480
NGC4261	0.0074	12h19m23.2s	+05d49m31s	2212
NGC5353	0.0078	13h53m26.7s	+40d16m59s	2325
NGC5846	0.0057	15h06m29.3s	+01d36m20s	1712
NGC5982	0.0101	15h38m39.8s	+59d21m21s	3017
NGC6658	0.0142	18h33m55.6s	+22d53m18s	4270
NGC7619	0.0125	23h20m14.5s	+08d12m22s	3762
Low-richness				
Galaxy	**Redshift**	**RA**	**DEC**	**Velocity (km/s)**
NGC0315	0.0165	00h57m48.9s	+30d21m09s	4942
NGC0524	0.0080	01h24m47.7s	+09d32m20s	2403
NGC1779	0.0111	05h05m18.1s	–09d08m50s	3313
NGC2768	0.0045	09h11m37.5s	+60d02m14s	1353
NGC3613	0.0068	11h18m36.1s	+58d00m00s	2051
NGC3665	0.0069	11h24m43.7s	+38d45m46s	2069
NGC5127	0.0162	13h23m45.0s	+31d33m57s	4862
NGC5490	0.0162	14h09m57.3s	+17d32m44s	4855
NGC5629	0.0150	14h28m16.4s	+25d50m56s	4498

[5] did a complimentary study on Brightest **Cluster** Galaxies (B**C**Gs), generally more massive and in denser environments than BGGs. It was found that there are two thresholds in the host clusters that determine whether star formation is allowed in the BCG. The two thresholds are the central entropy and the ratio of cooling-time (t_{cool}) to free-fall time (t_{ff}). We are interested in whether these or similar thresholds exist in X-ray rich groups.

The aim in this research is to constrain the SFH of BGGs. This can be done by classifying the galaxies as better described by a single stellar population (SSP) or a composite stellar population (CSP). According to [5] the convention is that most giant elliptical galaxies, such as the BGGs that is considered here, are passively evolving. Whether this holds true for BGGs, can be revealed by the SFH of the galaxies.

2. Method

2.1. Reduction

Since the data in the HET archive was not sky-subtracted, the first step was to do sky-subtraction. The data was then spatially binned into two bins - an inner bin (from 0 - 1 kpc) and an outer bin (from 1 - 2 kpc). This is done for each of the individual galaxies observed. This binning refers to binning along the spatial direction of the 2D spectra. This was done to ensure a high enough signal-to-noise ratio to have acceptable errors on the derived ages and metallicities.

2.2. ULySS

For the analysis, the stellar population code ULySS (University of Lyon Spectroscopic analysis Software) was used. The main routine in ULySS was used to compare the spectrum of a galaxy to the Vazdekis-MILES models [6] using all 985 stars.

The next step was to test the degree of the multiplicative polynomial. The multiplicative polynomial is used to subtract the continuum and dust as well as to account for any possible flux calibration differences between the galaxy and stellar template spectra. For this an SSP-fit was run for all 23 BGGs and for all MDs (Multiplicative Polynomial Degrees) between 1 and 30. After this, the resulting metallicity and age were plot against the different MDs. The optimal choice, where the solution converged, was a degree of 16.

Although the majority of stars inside the BGGs are believed to be old, we want to identify recent star formation episodes, by running both an SSP and a CSP fit for all 23 galaxies. This method is described in full in [5]. Thus, to accurately determine whether there is recent star formation in a galaxy, a CSP with two very different age components was chosen: a young component and an old component, even though no age or metallicity restrictions were placed on the two components.

The best way to do stellar population fitting is with a wide range of wavelengths, to break the age-metallicity degeneracy [7]. Due to some atmospheric features at the red-end of the spectrum (as can be seen in figure 1 and figure 2), the spectrum was truncated at 6200 Å, yielding a wavelength range of 4600-6200 Å, which is still wide enough for spectral fitting.

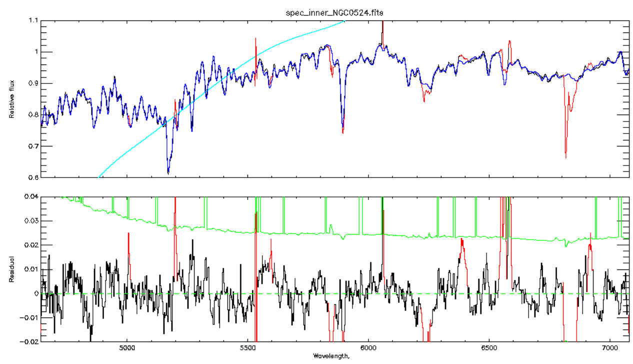

Figure 1. The spectrum of NGC0524 for the full observed wavelength-range. The black line indicates the observed spectrum, the blue line is the stellar population model of the best fit and the red is deviations that are masked during the fitting process. The light blue line shows the multiplicative polynomial that is used to normalize the continuum. The residuals are shown in the lower panel, where the green lines indicate the residuals as allowed by the error spectra (i.e. residuals larger than the green lines indicate deviations from the model as opposed to fluctuations caused by the noise in the spectrum).

ISBN: 978-0-620-85406-1

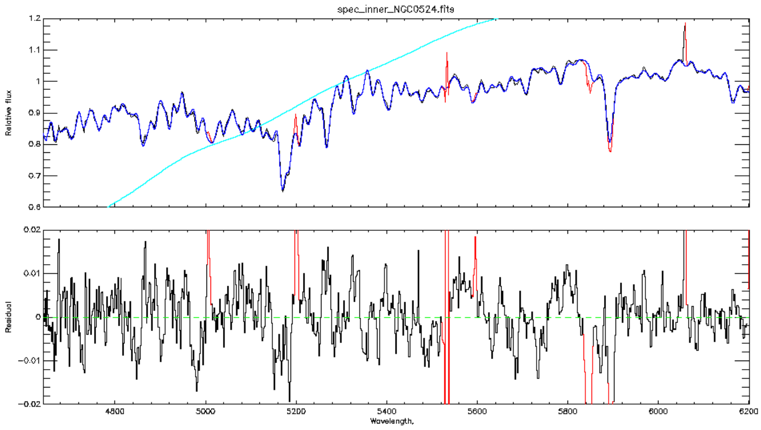

Figure 2. The same spectrum of NGC0524 as shown in figure 1, but now truncated at 4600-6200 Å. Thus, the atmospheric features are excluded.

3. Results and discussion

3.1. Classification

Table 2 gives a summary of the results obtained for both bins of all 23 galaxies.

Table 2. The results of the BGGs by using ULySS, indicating whether the bin was best fit by using a single or composite stellar population.

High-richness		
Galaxy	**Inner**	**Outer**
NGC0410	SSP	SSP
NGC0584	CSP	CSP
NGC0777	SSP	SSP
NGC0924	CSP	SSP
NGC1060	SSP	SSP
NGC1453	SSP	SSP
NGC1587	SSP	SSP
NGC2563	CSP	CSP
NGC4261	SSP	CSP
NGC5353	SSP	SSP
NGC5846	SSP	SSP
NGC5982	CSP	SSP
NGC6658	CSP	SSP
NGC7619	SSP	SSP

Low-richness		
Galaxy	**Inner**	**Outer**
NGC0315	SSP	SSP
NGC0524	CSP	SSP
NGC1779	CSP	CSP
NGC2768	SSP	SSP
NGC3613	SSP	CSP
NGC3665	SSP	SSP
NGC5127	SSP	CSP
NGC5490	SSP	SSP
NGC5629	CSP	SSP

In table 2 it is evident that some of the galaxies' inner bins are better described by a CSP while the outer bins are better described using an SSP. This is to be expected as the older stellar components mostly lie on the outskirts of the galaxy and the star formation mostly takes place in the central part of the galaxy (as is the case in NGC0924, NGC5982, NGC6658, NGC0524 and NGC5629). But, as is evident in NGC4261, NGC3613 and NGC5127, the inverse may also be possible (as described by [8] and [9]). For these three galaxies, it was found that the inner bin was best fit by a single population, while the outer bin was best fit by a composite population. Naively, one might expect recent star formation to occur in the central parts of the BGGs. However, it is possible that processes such as galaxy mergers or infalling satellites can lead to younger stars in the outer parts. Whether this is indeed the case here, needs to be further investigated by also looking at the X-ray and radio observations.

3.2. NaD
Figure 3 clearly shows a feature that is not well fitted by the model (around 5900 Å). The absorption line is that of NaD, which may be sensitive for the initial mass function (IMF), according to [10]. According to [11] this phenomenon can also be seen in dwarf galaxies. This remarkable discrepancy occurs in 14 BGGs and must be investigated further.

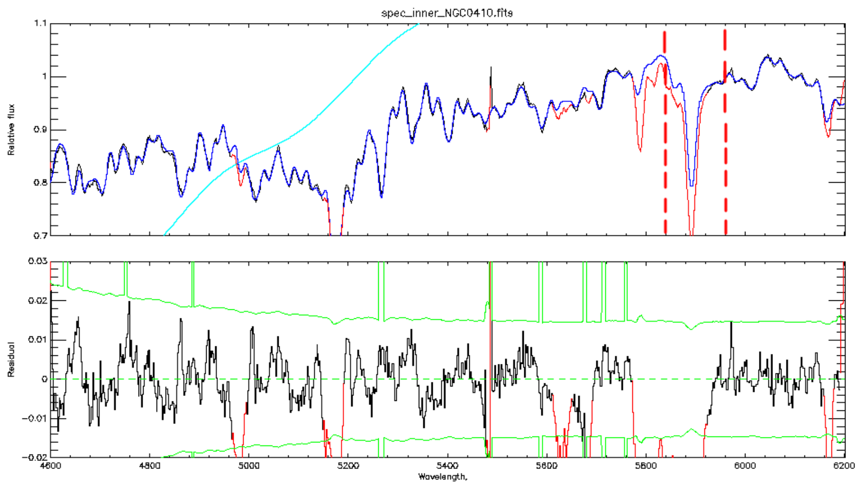

Figure 3. This is the spectrum of NGC0410. The NaD feature can be seen at 5900 Å (between the red dashed lines). The colours have the same meaning as in figure 1.

3.3. Brightest Cluster Galaxies
The same method was used in [5] for 32 BCGs to identify recent star formation episodes. Figure 4 (taken from [3], their figure 2a) shows the combined sample of 55 BGGs and BCGs. From this figure, it can be seen that the two populations, BGGs and BCGs, deviate in their Faber-Jackson relations. Now that we have star formation histories for all 55 central galaxies, these derived properties can be used to look for possible correlations between the galaxy and host group/cluster properties.

4. Conclusion and future work
The results obtained from the stellar population fitting now needs to be compared to data from other wavelengths (X-rays, radio, sub-millimetre, etc.). It is very important to verify why the galaxies which are better described by a CSP, had recent star formation episodes. The results can also be compared with the kinematic signatures of the galaxy groups [3]. After careful interpretation of the preliminary results presented here, we should be able to answer questions such as possible X-ray property thresholds for star formation in groups. Another important line of inquiry is to find out why there is a NaD overabundance as this may disclose some information of the IMF of the galaxies.

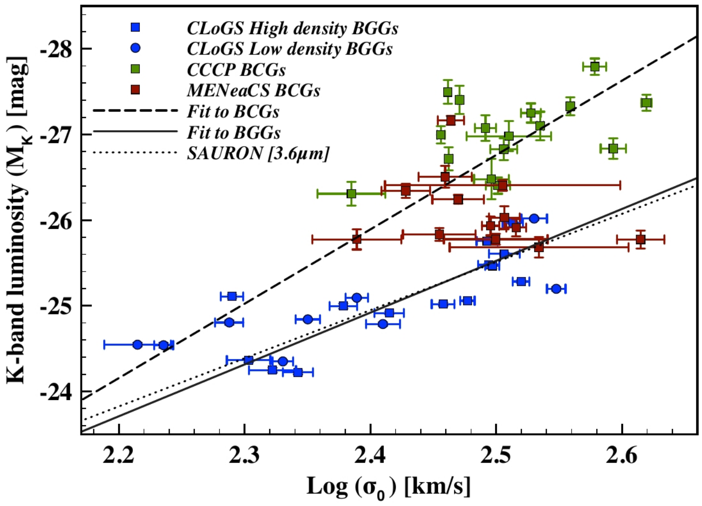

Figure 4. The BGGs are plotted in blue, while the BCGs are plotted in green and red. Note the two different Faber-Jackson relations (FJR) for the two classes. Figure from [3].

Acknowledgments
OCH is aided by the National Astrophysics and Space Science Programme (NASSP) and the National Research Foundation (NRF). SIL is aided by a Henri Chrétien International Research Grant administered by the American Astronomical Society and the NRF.

References

[1] Ponman T, Sanderson A J R and Finoguenov A 2003 The Birmingham-–CFA cluster scaling project – iii. Entropy and similarity in galaxy systems *MNRAS* **343** 331–42
[2] O'Sullivan E, et al. 2017 The Complete Local Volume Groups Sample - i. Sample selection and X-ray properties of the high-richness subsample *MNRAS* **472**(2) 1482–505
[3] Loubser S, Hoekstra H, Babul A, and O'Sullivan E 2018 Diversity in the stellar velocity dispersion profiles of a large sample of brightest cluster galaxies z $\leq$ 0.3 *MNRAS* **477** 335–58
[4] van den Bosch R C E, Gebhardt K, Gltekin K, Yıldırım A, and Walsh J L, 2015, Hunting for supermassive black holes in nearby galaxies with the Hobby-Eberly Telescope *ApJS* **218** 10
[5] Loubser S I, Babul A, Hoekstra H, Mahdavi A, Donahue M, Bildfell C, and Voit G M 2016 The regulation of star formation in cool-core clusters: Imprints on the stellar populations of Brightest Cluster Galaxies *MNRAS* **456** 1565–78
[6] Vazdekis A, Sánchez-Blázquez P, Falcón-Barroso J, Cenarro A J, Beasley M A, Cardiel N, Gorgas J, and Peletier R F 2010 Evolutionary stellar population synthesis with MILES i. The base models and a new line index system *MNRAS* **404** 1639–71
[7] Worthey G 1999 The age-metallicity degeneracy in spectrophotometric dating of stars and galaxies *ASPCS* **192** 283
[8] O'Sullivan E, Combes F, Hamer S, Salomé P, Babul A, and Raychaudhury S 2015 Cold gas in group dominant elliptical galaxies *A&A* **573** A111
[9] Davis D S, Mushotzky R F, Mulchaey J S, Worrall D M, Birkinshaw M, and Burstein D 1995 Diffuse hot gas in the NGC 4261 group of galaxies *ApJ*, **444**, 582–9
[10] Spiniello C, Trager S C, Koopmans L V E, and Chen Y P 2012 Evidence for a mild steepening and bottom-heavy initial mass function in massive galaxies from sodium and titanium-oxide indicators *ApJL* **753** L32
[11] Schwartz C M, and Martin C L 2004 A KECK/HIRES study of kinematics of the cold interstellar medium in dwarf starburst galaxies *ApJ* **610** 201–12